Performance analysis of Pareto optimal bearings subject to surface error variations

N. Bhat[a]

S.M. Barrans[b]

A.S. Kumar[c]

a. mpebnj@nus.edu.sg. National University of Singapore,
b. (corresponding author) s.m.barrans@hud.ac.uk. School of Computing and Engineering, University of Huddersfield, Queensgate, Huddersfield, HD1 3DH, UK. Telephone: +44 (01) 484 472407, Fax: +44 (01) 484 472252
c. mpeask@nus.edu.sg. National University of Singapore,

Abstract

A Pareto optimization study was carried out on a flat pad aerostatic bearing design. Some of the Pareto optimal configurations were then subjected to surface profiling errors including tilt, concavity, convexity and waviness and key performance parameters such as load capacity, stiffness and flow rate determined. From these studies it was concluded that multi-orifice aerostatic flat pad bearings are highly sensitive to surface profile variations and these surface profile variations are inherent limitations of the current manufacturing techniques. A technique to account for the sensitivity to manufacturing tolerance within air bearing optimization studies is also proposed.

Key Words: Pareto; surface; aerostatic; bearings

1. Introduction

The design of aerostatic bearings is becoming of increasing importance in engineering. As the trend to precision and ultra precision manufacture gains pace and the drive to higher quality and more reliable products continues, the advantages which can be gained from applying aerostatic bearings to machine tools, instrumentation and test rigs is becoming more apparent. Typical applications of aerostatic bearings are ultra precision diamond lathes [1], ultra precision 6 axis polishing machines [2], and coordinate measuring machines where highly repeatable positioning of one machine component relative to another is essential. These bearings are also used in micro-machines such as micro-turbo machinery [3] for their compactness and large power to weight ratio and a variety of other applications such as read/write heads of magnetic recording disks [4], extravehicular activity space suit [5] and nanometer resolution machines [6]. Air bearings offer a number of advantages over conventional bearings such as negligible wear and friction, high precision, silent and smooth operation, and physical and chemical stability, etc.

Aerostatic bearings are manufactured in a number of forms such a flat pad, spherical, conical, etc. Flat pad bearings are produced as both rectangular and circular devices and are often designed to be used in the externally pressurized, aerostatic mode where the effects of the relative motion of the

opposing surfaces on the air flow are insignificant. Externally pressurized air bearings may have a single entry orifice, multiple entry orifices or have a porous surface.

The literature presents a substantial amount of work done on the effect of manufacturing variations on the performance of the bearing. Early experimental and theoretical work by Pink and Stout [7] on aerostatic journal bearings demonstrated the effect of manufacturing errors on bearing performance. These errors included the position and diameter of the entry orifices and the form of the bearing surface. It was shown that such bearings were highly sensitive to deviations from the ideal cylindrical surface. Later work by Kwan and Post [8] considered the influence of manufacturing errors on a single type of multi-orifice, rectangular flat pad aerostatic bearings. Again, deviations of the bearing surface from the ideal plane had a significant effect on bearing load capacity, stiffness and air flow rate. Li and Ding[9] studied the influences of geometrical parameters of a pocketed type orifice restrictor on an aerostatic thrust bearing. Chen and He[10] investigated the performance of high-precision gas lubricated bearings and the effects of the recess shape, orifice diameter, gas film thickness, etc on the load capacity and flow rate. Sharma and Pandey[11] compared the performance of surface profiled(cycloidal, catenoidal and polynomial pads) hydrodynamic bearings with the conventional plane thrust bearings and concluded that cycloidal pads can carry more loads in comparison to other profiles of pad under study for the same inputs and also cycloidal pads generate about 30% more maximum pressure in the bearing compared to the conventional plane profile pad. Barrans et al[12] explored the manufacturing error sensitivity of Pareto optimal aerostatic bearings and concluded that the sensitivity of bearing stiffness in particular to form error could have a dramatic impact on bearing performance.

Currently typical flying heights for aerostatic bearings are in a range of 10 to 15 microns. However for nanometer applications, the gap height is much reduced and is of the order of three microns[13] with the minimum gap height permissible being very much dependant on the manufacturing techniques used. The most commonly used techniques for obtaining precisely finished flat surfaces for flat pad aerostatic bearings include grinding followed by more precise finishing operations like polishing/lapping [14]. Techniques like diamond turning [1] can also be used for obtaining flat surfaces with mirror finish which is ideal for flat pad bearing operation. Also improved grinding techniques like ELID grinding [15] and usage of micro-grinding tools[16] offer greater avenues for machining of precise flat pad bearing surfaces. In practice the maximum surface roughness allowed should not exceed 10% of the bearing clearance[17].

There have been various efforts to optimize the performance of gas bearings using various techniques. In particular global search techniques like GA's[18-19], simulated annealing[20] and direct algorithm[21,22] have been widely used. However, these procedures may be computational expensive due to a large amount of iterations involved. To overcome this and to speed up the optimization process, Bhat and Barrans[23] suggested the Pareto optimization technique using a uniformly distributed search technique. Wang et al[24] presented a performance evaluation of a new portable parallel programming paradigm, the Cluster OpenMP (CLOMP) for distributed computing, in conducting an optimum design of air bearings. The multi-objective optimization was carried out by using a genetic algorithm (GA) incorporating Pareto optimality criteria.

Although previous work[12] has been carried out to study the effect of manufacturing errors on the performance of multi-orifice flat pad bearings with different numbers of entry, a detailed study on how it affects the operational performance of the bearing and inherent limitations in the current techniques is lacking. In this paper a validated FEA (Finite Element Analysis) code[23] has been used to examine the effects of surface form errors. A number of different Pareto optimal bearing types are examined and the relative sensitivity of these bearings to manufacturing errors is investigated in terms of operating performance of the bearing. Current manufacturing techniques for air bearings are also investigated and the concept of a performance volume has been introduced to include manufacturing error sensitivity within the optimization process.

2. Background Study

2.1 Pareto optimality criteria

The optimization of aerostatic flat pad bearings is considered from the viewpoint of maximizing the load and stiffness and minimizing the flow rate. Since conflicting criteria are involved in this case, the Pareto optimal concept is used to identify the optimal solution sets. The Pareto optimum set is defined as a non-inferior set of solutions for which there is no way of improving any criterion without worsening at least one other criterion. The technique of identifying the Pareto optimal set of bearing designs by comparing the performance of the bearings over a feasible range of gap heights has been demonstrated by Bhat and Barrans[25]. It is noted that at present, the optimization does not take into account choking of the flow and considers only the static stability of the bearing.

The content of the Pareto set will clearly depend upon the constraints placed on the design variables for a particular application. For the purposes of this paper, a Rank L inherently compensated bearing of the form (similar to the one used in [12]) shown in Figure 1 was used with the constraints shown in Table 1. However in this case a fixed feed pipe length was used rather than a fixed feed pipe diameter as is the case of [12]. This eliminated bearing designs with long pipes. Thus orifice diameter dominates the inlet flow resistance unlike the case of [12] where orifice length is the major restrictor to the inlet flow into the gap. This makes the bearing easier to manufacture and assemble than the ones in [12] where long feed pipes have to be assembled into the bearing.

As in the previous work [12] variable rather than fixed orifice spacing along the length of the bearing was used to extend the high pressure region under the bearing and hence increase load capacity. In this optimization problem, the objective is to minimize all the three performance criterion values, so the original problem of optimizing different criterion (maximize(load, stiffness), minimize(flow)) changes to minimize(1/Load,1/stiffness, flow). Hence high performance is associated with low values of the criteria shown here.
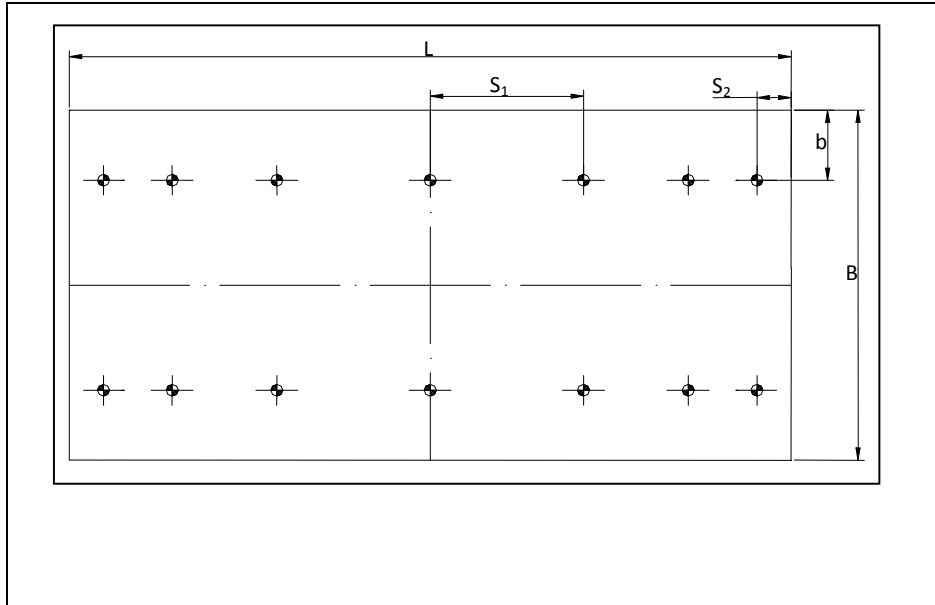
Figure 1. Design variables defining the Rank L bearing configuration used for
this study

The optimization run was carried out using an experimentally validated code developed by Bhat and Barrans[23]. The elements used to model the air gap were two dimensional linear elements with a formulation derived from the Reynolds equation for steady state, laminar flow between parallel plates. An automatic mesh generation package was used to define up to six elements between orifices. The inlet orifices were modeled using linear one dimensional elements simulating flow through a long pipe.

Input Variable	Range	Input Variable	Range
Aspect Ratio (L/B)	1 – 2	Number of orifices along length	3 - 10
Breadth of bearing (B)	60mm – 75mm	Orifice spacing ratio (S_1/S_2)	1 - 3
Side land ratio b/B	0.1 – 0.25	Diameter of orifice	0.05 – 1 mm
Supply Pressure value	4 bar – 6 bar	Length of orifice	10 mm

Table 1. Design variable ranges

2.2 Surface profiling errors

Manufacturing error variations as characterized by Kwan and Post[8] are shown in Figure 2. These consist of tilt, sinusoidal concavity or convexity in one dimension and waviness in one dimension. Waviness can be further subdivided based on the number of wavelengths appearing over the length of the bearing, as shown in Figure 2. Clearly, this list is not exhaustive but will include the frequently occurring errors.
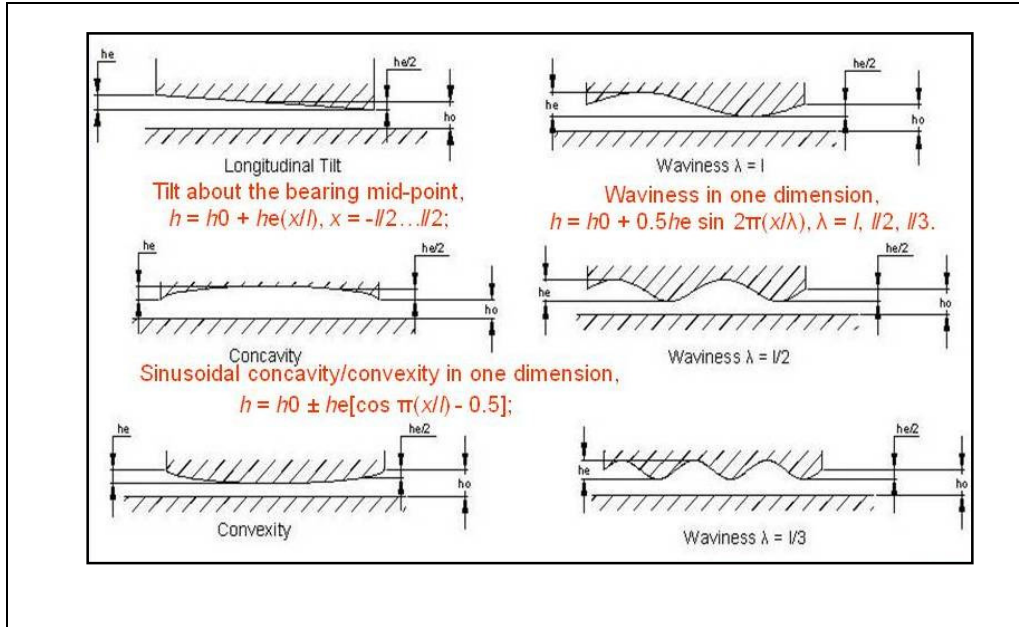
Figure 2. Nominal gap height, h_0 and error magnitude, h_e, for the six surface error forms being considered

It can be seen that the gap height is a function of he(maximum error deviation) and ho(nominal gap height) depending on the type of error wave form(tilt, concavity, etc). The validated finite element code developed by Bhat and Barrans[23] was extended to allow these variations to be included. This finite element code models the air gap assuming that there is steady state, compressible, laminar flow between surfaces that are locally parallel. The flow resistance offered by the orifices is introduced using a pipe element of the required length and diameter. Previous studies [23] had indicated that 400 to 500 elements modeling a quarter of the bearing were sufficient to provide a converged solution.

The form error was defined as a function of nominal gap height and its variation is as shown in Table 2. Thus unlike [12] a fixed form error value rather than variable one was used. This helps in quantifying the performance of the bearing with respect to the change in form error value and compares the performance of different bearing configurations on a common scale.

h_e/h_0	0.065	0.133	0.267	0.4	0.533	0.667	0.8	0.915
h_e(microns) (based on h_0 = 5 microns)	0.325	0.665	1.335	2	2.665	3.335	4	4.575

Table 2 Form error magnitudes used in this study

3. Pareto Optimization Studies

A Pareto optimization study akin to the one described earlier by Bhat and Barrans[23] was carried out based on the input parameters given in Table 1. The criteria used in the study were not simply the values of load, stiffness and flow at a particular gap height. Rather, as described in detail in [25], these performance values were determined over a range of gap heights between acceptable limits. The area

under this performance curve was then used as the criterion in each case. This concept of a performance area is discussed in more detail in section 7.

The results of the Pareto optimization run are given in Table 3. The design numbers here are simply references to a uniformly distributed sequence of points within the design space. The Pareto optimal points are selected from the trial points by comparing the performance criteria of all points. Those points that cannot be improved on with respect to one criterion without worsening at least one other criterion are members of the Pareto set. Only the Pareto optimal points are given in Table 3.

Design No.	Bearing aspect ratio L/B	Bearing width B(m)	Side land ratio b/B	N° orifices n	Orifice spacing ratio S1/S2	Pressure ratio	Orifice pipe diameter (mm)	1/Load Area (1/Nμm^2)	1/Stiff Area (N)	Flow Area (kgμm/s)	Rank
143	1.94	0.072	0.224	3	1.23	5.5703	0.3877	3.89E-05	6.64E-02	2.02E-03	1
107	1.84	0.070	0.283	7	2.42	4.8594	0.0871	4.76E-05	6.90E-04	1.85E-03	2
25	1.59	0.075	0.219	3	1.31	5.3125	0.3766	4.33E-05	6.25E-02	2.11E-03	3
211	1.79	0.067	0.298	6	2.49	5.7734	0.0834	4.92E-05	6.59E-04	2.03E-03	4
231	1.90	0.065	0.182	8	2.40	5.6797	0.0686	6.66E-05	5.72E-04	1.47E-03	5
235	1.84	0.070	0.145	4	1.52	5.5547	0.2467	4.55E-05	1.20E-02	2.72E-03	6
7	1.88	0.073	0.225	4	1.75	4.75	0.6438	3.82E-05	4.07E-01	3.01E-03	7
93	1.73	0.064	0.298	5	2.52	5.9531	0.1020	4.34E-05	8.18E-04	3.18E-03	8
199	1.89	0.068	0.191	4	2.80	5.8359	0.1725	4.22E-05	2.94E-03	3.25E-03	9
155	1.85	0.071	0.131	5	2.91	5.5078	0.2986	4.15E-05	2.33E-02	3.27E-03	10
190	1.49	0.070	0.196	6	2.76	4.6016	0.0760	9.64E-05	9.49E-04	9.92E-04	11
185	1.61	0.071	0.271	5	2.01	5.8516	0.4322	3.35E-05	1.09E-01	3.45E-03	12
195	1.76	0.074	0.216	4	1.55	5.5859	0.7662	3.66E-05	9.87E-01	2.68E-03	13
78	1.45	0.075	0.167	5	1.08	4.2656	0.0723	1.09E-04	9.42E-04	6.02E-04	14
113	1.55	0.067	0.177	8	2.48	5.4219	0.0574	1.14E-04	7.10E-04	7.29E-04	15
77	1.70	0.071	0.217	3	1.58	5.7656	0.7848	4.50E-05	1.35E+00	1.94E-03	16
45	1.70	0.073	0.103	6	1.22	5.2188	0.3617	4.08E-05	4.61E-02	4.04E-03	17
137	1.57	0.067	0.199	6	1.48	5.8203	0.2689	3.91E-05	1.85E-02	4.24E-03	18
133	1.63	0.062	0.237	10	2.35	5.9453	0.0908	4.30E-05	7.48E-04	4.35E-03	19
111	1.96	0.064	0.258	6	1.67	5.1094	0.4434	3.53E-05	1.05E-01	4.57E-03	20
203	1.82	0.073	0.154	7	1.93	5.7109	0.3506	2.93E-05	3.69E-02	4.68E-03	21
238	1.46	0.072	0.220	7	1.77	4.8047	0.1279	3.87E-05	1.19E-03	4.60E-03	22
167	1.89	0.070	0.277	6	2.45	5.2891	0.6994	3.09E-05	6.06E-01	4.43E-03	23
15	1.94	0.072	0.163	6	2.13	4.875	0.2281	3.30E-05	5.73E-03	4.88E-03	24
255	2.00	0.072	0.201	5	1.71	5.9922	0.8701	2.97E-05	1.48E+00	3.19E-03	25
27	1.84	0.071	0.269	8	1.81	4.8125	0.1391	2.90E-05	1.17E-03	5.80E-03	26
119	1.93	0.073	0.202	6	2.23	5.1719	0.1762	2.77E-05	1.96E-03	5.88E-03	27
97	1.52	0.074	0.295	7	1.55	5.2344	0.7402	2.81E-05	7.68E-01	5.62E-03	28
135	1.88	0.073	0.287	7	2.85	5.4453	0.8033	2.47E-05	9.58E-01	6.01E-03	29
69	1.63	0.072	0.280	8	1.20	5.6406	0.2504	2.57E-05	1.03E-02	6.51E-03	30

227	1.78	0.071	0.207	9	1.15	5.4297	0.6623	2.54E-05	4.45E-01	6.85E-03	31
165	1.64	0.074	0.227	7	1.95	5.7891	0.9369	2.75E-05	2.02E+00	4.91E-03	32
247	1.93	0.073	0.263	10	1.34	5.8672	0.3357	1.99E-05	2.75E-02	7.62E-03	33
171	1.83	0.075	0.240	9	1.57	5.1641	0.8775	2.22E-05	1.15E+00	7.16E-03	34
151	1.91	0.066	0.168	9	1.79	5.6328	0.1205	2.86E-05	7.41E-04	7.75E-03	35
152	1.10	0.067	0.181	4	1.41	5.0078	0.0611	2.26E-04	1.40E-03	3.90E-04	36
193	1.51	0.062	0.166	6	1.05	4.0859	0.0537	2.85E-04	1.55E-03	2.22E-04	37
75	1.82	0.073	0.292	10	2.83	5.0156	0.1910	2.22E-05	2.66E-03	1.03E-02	38

Table 3 Design variables and performance values for the generated Pareto set

The content of the Pareto set will clearly depend upon the constraints placed on the design variables as shown in Table 1 for a particular application. Moreover, high performance is associated with low values of the criteria shown here. The Pareto optimal points were ranked based on a weighting method previously described by Barrans and Bhat [25],which places the points in order based on their distance from the origin in normalized criteria space. It should be noted here that only the Pareto set is ranked so all points are still Pareto optimal. The ranking process simply serves to identify those designs where performance with respect to one or two criteria is not extreme. The normalized result which illustrates the performance of different Pareto optimal points is shown in Figure 3.
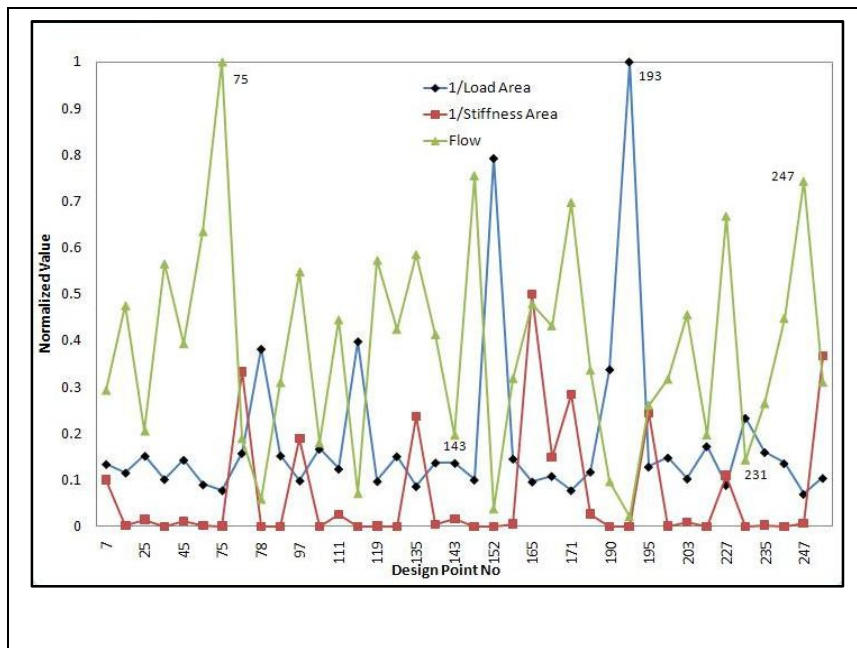
Figure 3: Relative performance of Pareto optimal set

The compromises associated with bearing design are clearly illustrated by these results. Design 75 has the high stiffness and a high load capacity but also has the highest flow rate which affects its ranking in the Pareto optimal set. Design 193 minimizes the flow rate but this significantly reduces the load capacity. Point 143 provides the best compromise between all three criteria and hence is ranked number

one in the Pareto set of optimal designs. The design parameter values for these designs are shown in Table 3. Point 231 has the highest stiffness but also a very high flow rate. Similar is the case for point 247 which has the highest load capacity but its position in the ranking table is affected on account of having high flow rate values.

4. Performance changes

In this section, the change in performance characteristics for a Pareto optimal bearing is analyzed for various surface profiles. Pareto optimal bearing 119 with dimensions as given in Table 3 is chosen for analysis. Figure 4 shows the impact of three of the form errors on the three performance criteria. Figure 4(a) shows the effect of a concave surface profile on stiffness. The stiffness, K, has been normalized with respect to the nominal load capacity K_n (i.e. load capacity at that particular gap height with no manufacturing error) on the vertical axis. At low gap heights, an increasing magnitude of concavity error (he) gives a large increase in stiffness values(K/K_n~6). Stiffness is a complex mechanism involving two resistances in series (resistance due to the orifice and resistance due to the gap height). It is maximized when the two resistances have almost the same value. Introducing concavity to the bearing surface makes the resistance to air flow more complex. At low gap heights with a high level of concavity, there are effectively three resistances: the feed pipe or orifice, the gap region in the centre of the bearing where the resultant gap is large and the gap region towards the ends of the bearing where the resultant gap is small. This third resistance is over only a small length of bearing. Hence, a small change in gap height here will have a dramatic effect on the air resistance and hence the stiffness. Longitudinal concavity also results in an increase in the load capacity of the bearing, specifically at lower gap heights as seen in Figure 4(c). This effect has already been explained in the previous section. However, this effect is not significant at higher gap heights due to increased flow rates, which results is rapid pressure loss just beneath the orifice. This effect is also referred to as the pressure depression effect [26]

However, if manufacturing errors result in longitudinal convexity of the bearing surface, it can have deleterious effects on the stiffness as shown by negative stiffness regions in Figure 4(b). Although this phenomenon has been mostly attributed to journal aerostatic bearings[27], It has also been observed in flat pad aerostatic bearings[28]. It can be seen from the graph that it occurs at low values of gap heights and for maximum allowable value of surface deviation. This effect is often termed static instability or 'lock up' which commonly occurs for orifice compensated bearings [28-31]. The negative stiffness region implies that bearings will support a lower load as the gap height closes than what it will support at higher gap heights.
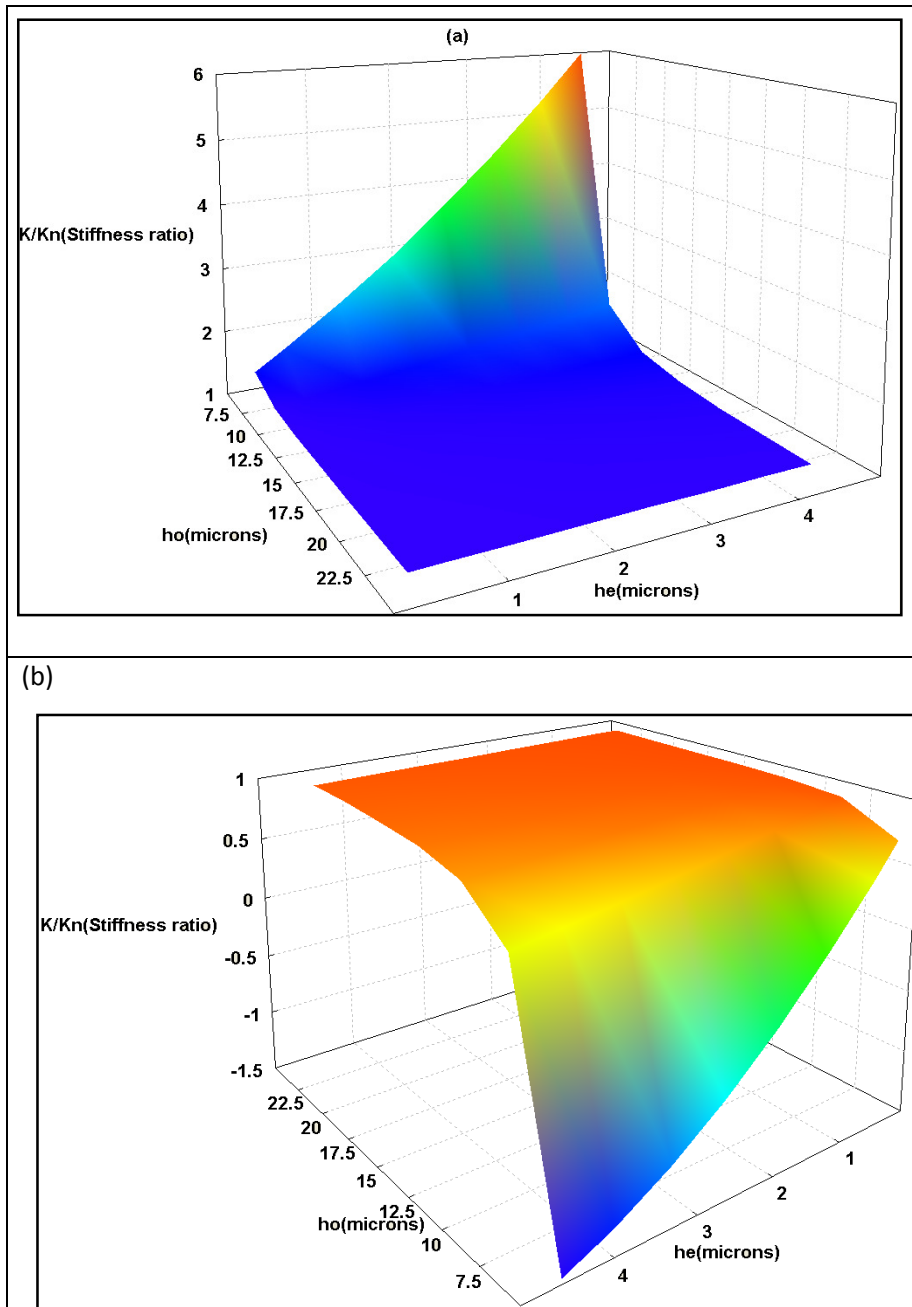
Figure 4 Performance characteristics over the range of nominal gap heights, h_0, and error magnitudes, h_e, for Pareto optimal bearing 119 ((a) stiffness, concave error, (b) stiffness convex error
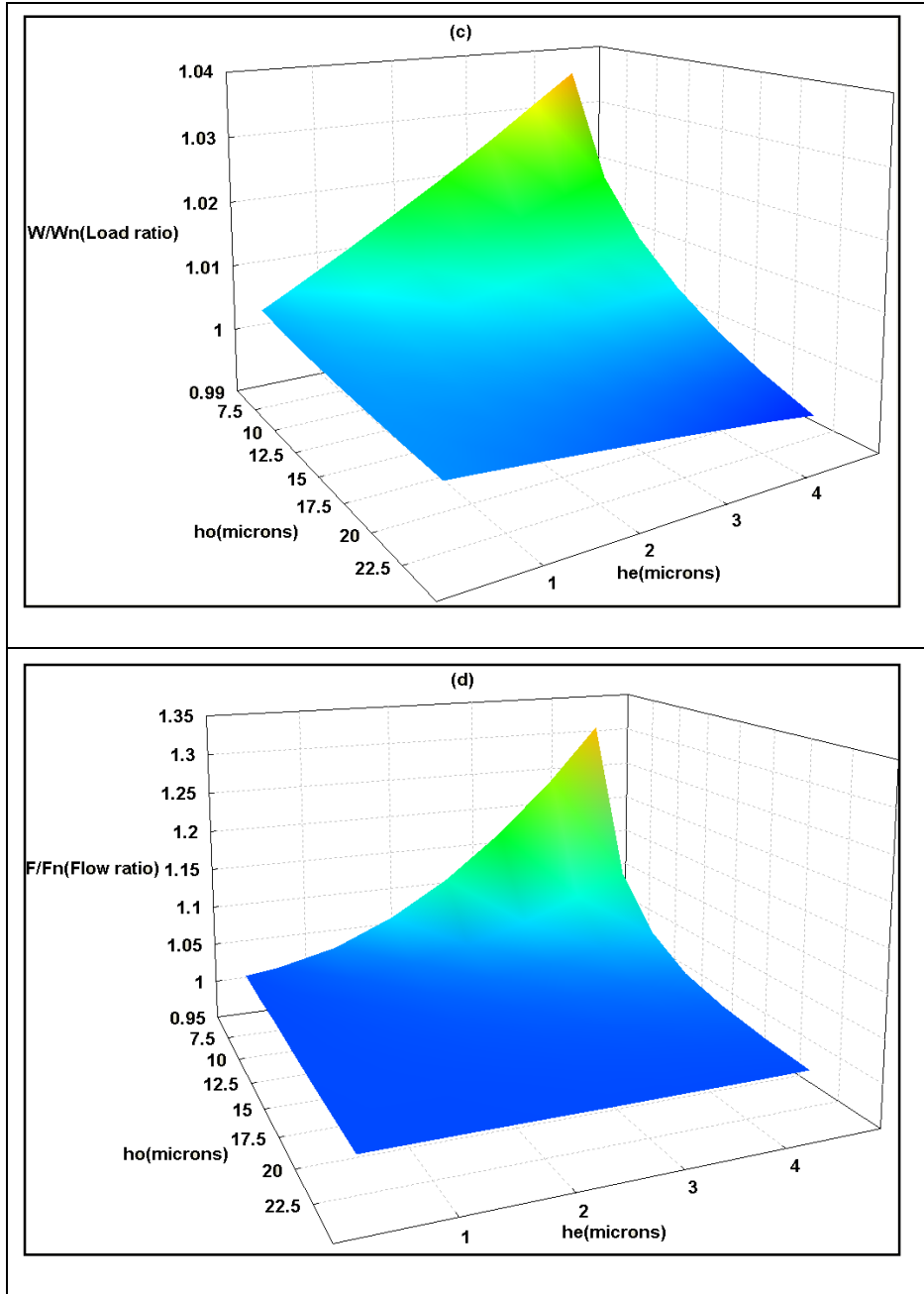
Figure 4 Performance characteristics over the range of nominal gap heights, h_0, and error magnitudes, h_e, for Pareto optimal bearing 119 ((c) load,concave error, (d) flow, sinusoidal error)

This trend can be clearly seen from Figure 5 wherein the load capacity actually decreases at smaller gap heights (h~<6 microns) giving rise to negative stiffness regions.
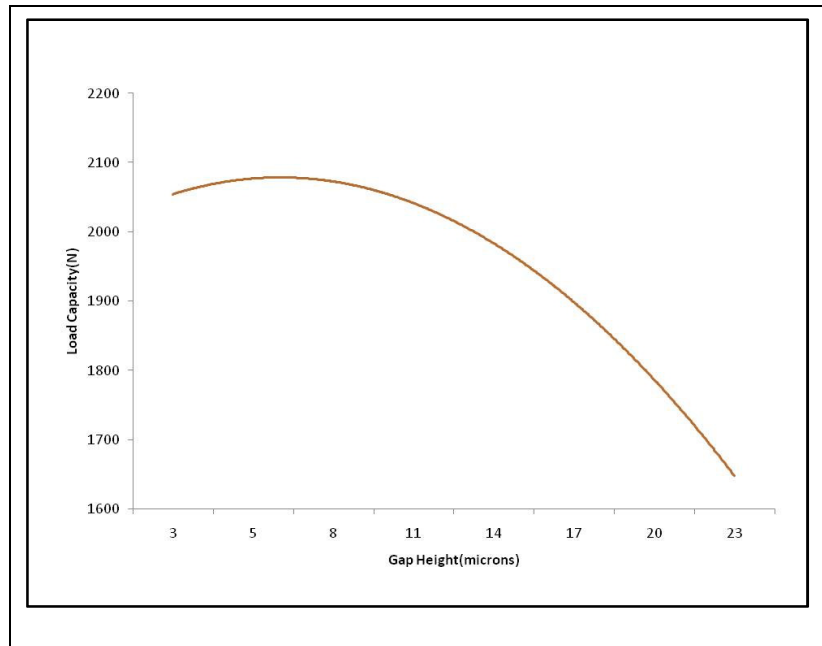
Figure 5 Load capacity variation with nominal gap height, h_0, for
design 119 (Convex surface profile and maximum value of form
error h_e)

Lock up has been attributed to unevenness in the flow distribution among the feeder holes due to manufacturing inaccuracies or faulty design[29]. However, in the cases shown here the negative stiffness is generated when the orifice pressure approaches the supply pressure. Further reduction in the air gap can therefore not be accompanied by an increase in pressure in the air gap and hence there is no increase in load capacity. Where the air gap is uneven, this effect will vary from orifice to orifice. This is the case for bearing number 119 since multiple orifices are distributed in accordance with the spacing ratio along a convex surface leading to uneven flow between different orifices due to varying gap heights. The effect is also a function of orifice spacing ratio since this influences how the orifices are placed along the manufactured surface. Orifices closer to the edge will leak more as compared to the orifices near the center of the bearing. It can be seen from Figure 6 that the negative stiffness region disappears as the orifice spacing ratio is increased to 3 from a current value of 2.2 since there is less unevenness in flow distribution as all the orifices are located towards the edge of the bearing. It can be also seen from figure 4(b) that with the increase of gap height the effect of surface unevenness is minimized and hence the negative stiffness regions are eliminated.

Figure 4(d) illustrates the relation between the sinusoidal form error(Waviness = L/2) and flow rate. The rate of increase of flow rate is greater for smaller values of gap heights with increasing value of sinusoidal form error. However for higher values of gap height there is no significant increase in flow rate values as the surface variations do not significantly alter the resistance across the gap at higher values of gap heights.

Thus at higher gap heights, these curvature errors do not play a significant role in altering the flow profile in an aerostatic flat pad bearing.
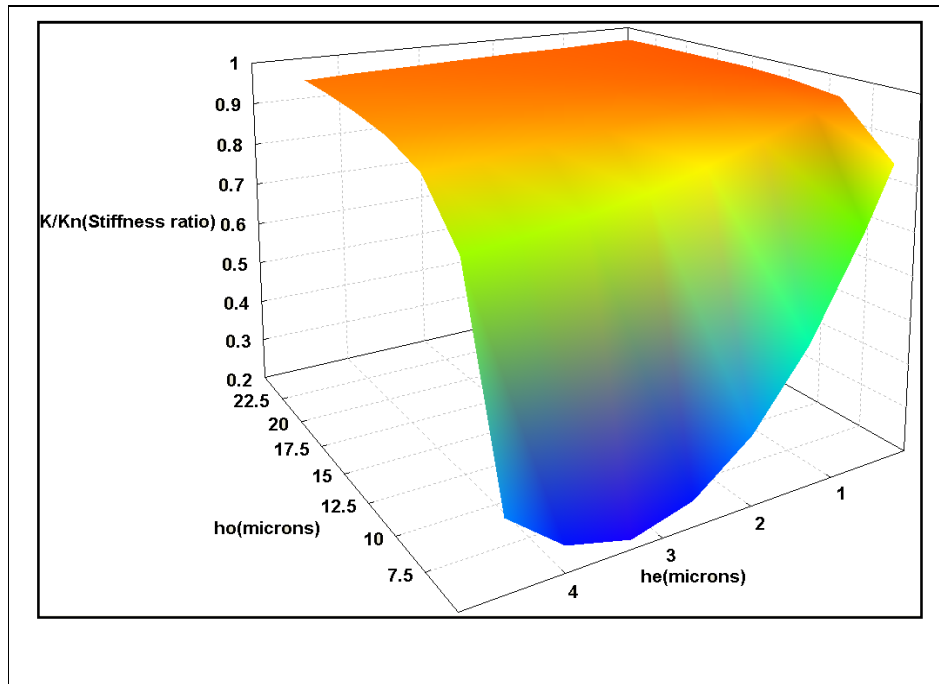
Figure 6 Change in stiffness for design 119 over a range of nominal gap heights, h_0, and magnitudes, h_e, of convex surface form error.

5.   Change in operating gap height

Surface variations along the surface of the air bearing can either improve or impair the performance of the bearing as seen in section 4. Apart from negative stiffness regions as shown in section 4, surface variations can also lead to a drop in load capacity and increase in flow rates for certain values of gap heights. Thus it is necessary to understand the change in operating performance of the bearing when it is subjected to surface variations.

Three Pareto optimal bearing designs as identified in Figure 3(143, 75 and 193) were selected to analyze their performance based on sensitivity error analysis. Whilst Point 143 gives a good compromise in terms of load capacity, stiffness and flow rate, Point 193 has the lowest flow rate while Point 247 has the highest load capacity over a range of gap heights.   The maximum and minimum change in performance over all six form errors were identified for each performance criterion for the full range of operating gap height. The results of this analysis are shown in table 4.

Design	W/W$_n$		K/K$_n$		F/F$_n$	
	max	min	max	min	max	min
143	1.131	0.864	46.744	-46.18	1.88	0.543
247	1.04	0.96	17.01	-5.5	1.32	0.99
193	1.10	0.88	1.18	0.5	1.21	0.79

Table 4. Typical ranges of changes in performance characteristics
for different Pareto optimal bearing designs

It is clear from these results that load capacity is the performance criterion least affected by form error. Form error had the least impact on load capacity for design 247, the bearing that was selected as having a particularly high load capacity. Design 193 which was selected because it had a low flow rate, showed the least sensitivity to all three form errors. It was interesting that whilst design 143 gave a good compromise in terms of the performance criteria, design 193 out performs it in terms of sensitivity to form error, although design 193 was ranked 37 places behind point 143 as can be seen in Table 3. Both point 143 and 247 have negative stiffness regions as can be seen from Table 4. This makes both the bearing designs extremely sensitive to form errors.

Of all the three form errors, it can be seen that stiffness is the most impacted when the bearing is subjected to surface deviation errors. This affects the operating gap height for the bearings since the bearings are no longer functional at those gap heights due to negative stiffness or due to the bearing stiffness values being much below the rated stiffness value at those operating gap heights. Figure 7(a) shows the performance for bearing 247(selected for highest load capacity) at a gap height of 5 microns for various values of convexity surface error deviation whilst Figure 7(b) shows the performance for bearing 193 at a gap height of 5 microns for various values of sinusoidal surface error deviation(wavelength = l)

It can be seen for both the cases that the bearing is virtually inoperable for a gap height of 5 microns. In case of bearing 247, it is due to the presence of negative stiffness region whilst in the case of bearing 193; the actual values of stiffness and load capacity are much lower than the nominal values. This example highlights the importance of using the manufacturing error sensitivity as a performance criterion in an air bearing optimization problem since manufacturing variations can drastically affect the operating range of an air bearing.
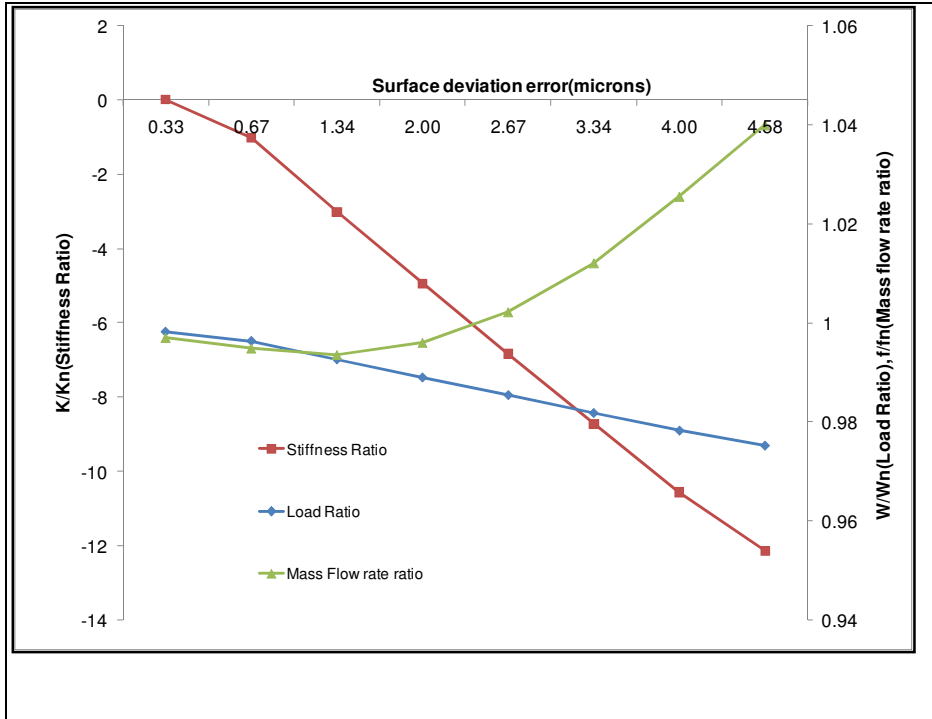
Figure 7(a) Impact of convexity error magnitude on load capacity, stiffness and flow for bearing 247at a gap height of 5 microns
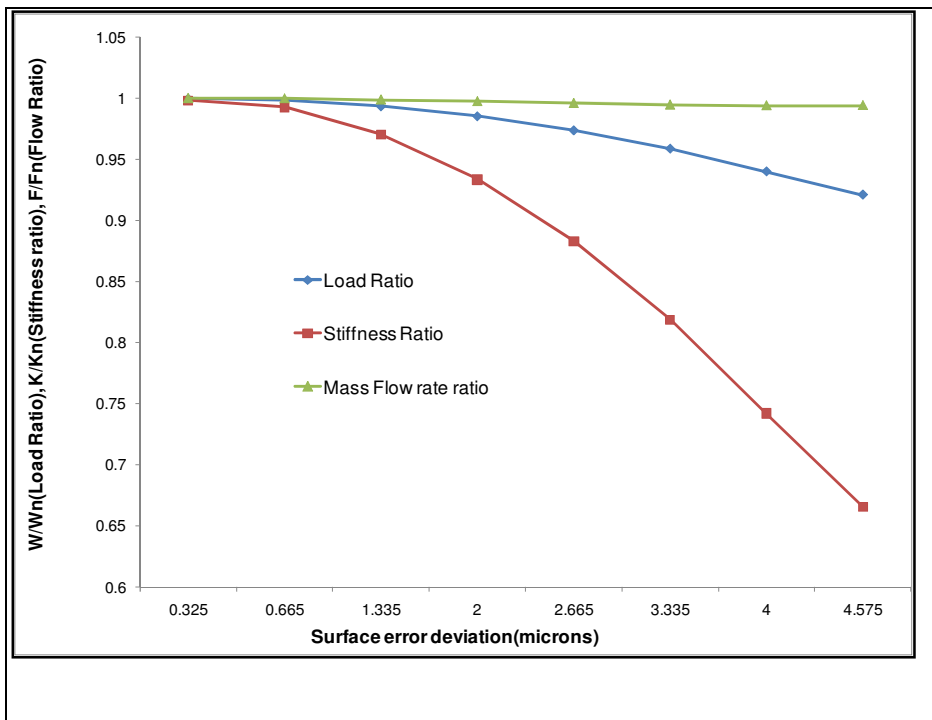
Figure 7(b) Impact of sinusoidal (wavelength = l) error magnitude on load capacity, stiffness and flow for bearing 193 247at a gap height of 5 microns

6. Current surface manufacturing methods and their relevance for flat pad bearing manufacture

In the previous sections the effect of form errors on the performance of multi-orifice bearings was highlighted. Whilst in some cases the surface variations can enhance the performance of the bearing, it can also cause a sudden loss in stiffness as seen in section 5. Thus surface accuracy and flatness of air bearing pads become a significant factor and needs to be accurately controlled. As stated before maximum surface roughness should not exceed 10% of the bearing clearance. Ultra precision machining techniques which remove materials from a few microns to sub-micron level like diamond turning[1] and finishing processes like ELID grinding and lapping/polishing[14,15] can be used to machine air bearing surfaces with sub micrometric form accuracy and nanometric roughness. Diamond turning is an ultra-precision lathe-like process using a single point diamond tool predominantly used on ductile materials (metals, plastics etc). It is particularly useful in producing flat, spherical and aspheric mirrors, off-axis and free-form surfaces. This machining process is able to achieve mirror surface finish of less than 10 nm roughness and form error of less than 1 µm [32].However, a big challenge posed is the short tool life of diamond cutters and polishing process like lapping are often required after diamond turning since the diamond turning process leaves a regular pattern of "diamond turning marks" on the surface[33].

A commonly used polishing technique is manual lapping [34], which uses a precisely shaped rigid lap made of pitch or polyurethane. This transfers pressure through abrasive slurry to the entire surface material of the component. Material is then removed by chemical and mechanical interactions between the abrasive and the component. However, it has a relatively slow removal rate and so takes a long time to fabricate high precision surfaces. Automated lapping using 6 axis polishing machining system with sub-aperture lapping and on-line testing capability has also been reported[35]. The new system is based on computer-controlled optical surfacing (CCOS), which combines the faculties of grinding, polishing, and on-machine profile measuring, and has the features of conventional loose abrasive machining with the characteristics of a tool having multiple degrees of freedom.

ELID grinding[32] can also be used for nanosurface generation since it improves over the conventional grinding process. The latter produces a poorer finish because the active sharp grits per unit area of the grinding wheel decreases during grinding until the next dressing cycle. In the case of the ELID grinding technique, the active sharp grits per unit area of the wheel remain the same due to constant dressing and this leads to improved surface integrity and surface roughness. The ELID grinding technique also has the advantage of reducing the bonding strength of the wheel working surface, hence improving grindability.

Ultraprecision mirror surface grinding using ELID, which achieved a surface roughness of 0.007 microns in Ra and surface straightness of 0.25 microns for a metal mold steel has been reported[36]. Commercially available system like the Zeeko polishing machine [37] have been gaining prominence. Although this machine was originally designed to manufacture aspheric glass telescope lenses, Charlton et al[38,39] have demonstrated that the machine can also be used to effect the removal of surface material from a range of materials and the depth of material removal can be controlled to a precision of less than 100 nm, dependent on the material being machined and the polishing media being used for

the removal. A shallow pocket of about 4 μm depth for a novel aerostatic flat pad bearing was machined using this process[40]. Precision profiled surfaces[41] can also be manufactured using this machine. This feature can be used to manufacture high performance flat pad bearings with engineered surface profiles that enhance bearing performance as seen in the previous sections. However the disadvantage of the process is that the processing time is very long and deviations in shapes caused due to limitation of polishing head radius [40].

7. Concept of performance volume

The previous optimization studies [23, See section 3] carried out consider the areas under the load, stiffness and flow curves for a flat pad bearing as performance criteria wherein the objective is to maximize the load and stiffness areas whilst minimizing the flow area. This is done by calculating the load, flow and stiffness characteristics over the full range of gap heights. This methodology was employed because it was recognized that a flat pad bearing will operate over a range of gap heights depending on the load applied. Whilst at a specific gap height performance may be very good, at another height an aspect of performance may be very poor. However as seen from the previous section load, stiffness and flow are highly sensitive to bearing surface deviations. Therefore in order to ensure robust bearing performance, it is necessary to incorporate the effect of different types of surface error profiles over the full range of operational gap heights into the optimization study.

Herein we propose the concept of performance volume to account for manufacturing variability within an optimization process. The performance volume concept helps in selection of bearings which are not just optimized in terms of performance criteria[23] but are also relatively insensitive to manufacturing variations. In [23] the lower and upper limit for calculating the areas under the load, stiffness and flow curves (based on predefined bearing performance) in Figure 8 was derived as follows.

$$L_L = max(\, h_{min}, h_2 \,) \dots\dots\dots\dots\dots\dots\dots\dots\dots\dots\dots\dots\dots \text{Eqn 1}$$

$$U_L = min(\, h_1, h_3, h_4 \,) \dots\dots\dots\dots\dots\dots\dots\dots\dots\dots\dots\dots\dots \text{Eqn 2}$$
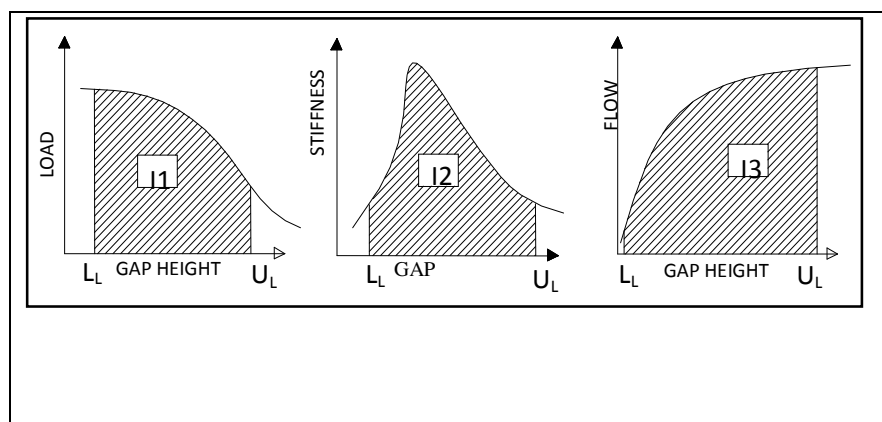
Figure 8. Performance area curves

Wherein h_1 is the gap height where the minimum load condition is reached, h_2 and h_3 are the gap heights where the minimum stiffness condition is reached and h_4 is the gap height where the maximum flow condition is reached. h_{min} being the minimum gap height based on the surface tolerance grade for the bearing [23].

A similar process would be involved when the performance of the bearing subject to surface error deviation is considered. However in this case the performance curves for a bearing subjected to surface error deviation will have to be considered. For example the maximum load capacity (max load over tolerance range) will be the maximum load over 6 different ranges of surface deviations (tilt, concavity, convexity, etc) subjected to varying surface deviation values for that particular gap height. This has been illustrated in Table 5 which shows the maximum and minimum load capacity over a range of surface error deviations and tolerance range values. Performing these calculations over a range of gap heights and range of surface error deviation values would generate performance area graphs as shown in Figure 9. This would enable the lower(L_L) and the upper limit(U_L) over which the performance of the bearing needs to be assessed to be defined.

Having calculated the lower and the upper limits, the performance volume between the lower and upper limit over a range of surface error forms and magnitudes can be calculated. For example, table 5 shows the load capacity for a nominal gap of 5 mm for each of the six surface error forms over a range of surface error magnitudes. For each error magnitude, one of the error forms will result in the lowest load capacity. Plotting these minimum load capacities over a range of nominal gaps will result in graphs of the form shown in figure 10. The volume under this graph between the previously identified upper (U_L) and lower (L_L) limits will provide a measure of the performance of the bearing. Three performance measures can thus be defined accounting for manufacturing variability and used in the Pareto optimization routine.

Form error magnitude(µm)	0.325	0.665	1.34	2.00	2.67	3.34E	4.00	4.58
Load Capacity(gap = 5 µm)								
Longitudinal tilt	671.81	671.85	671.99	672.23	672.55	672.98	673.52	674.09
Concavity (sinusoidal)	672.48	672.88	672.82	671.69	669.59	666.56	662.72	658.77
Convexity (sinusoidal)	**670.82**	**669.48**	665.78	660.69	654.11	645.91	636.19	626.50
Waviness (sinusoidal)								
λ = l	671.54	670.72	667.42	661.93	654.17	643.99	631.45	618.59
λ = l/2	671.37	669.99	**664.55**	**655.63**	**643.36**	**627.80**	**609.40**	**591.28**
λ = l/3	671.48	670.46	666.37	659.58	650.02	637.56	622.42	607.12

Table 5 Example illustrating calculation of minimum load capacities
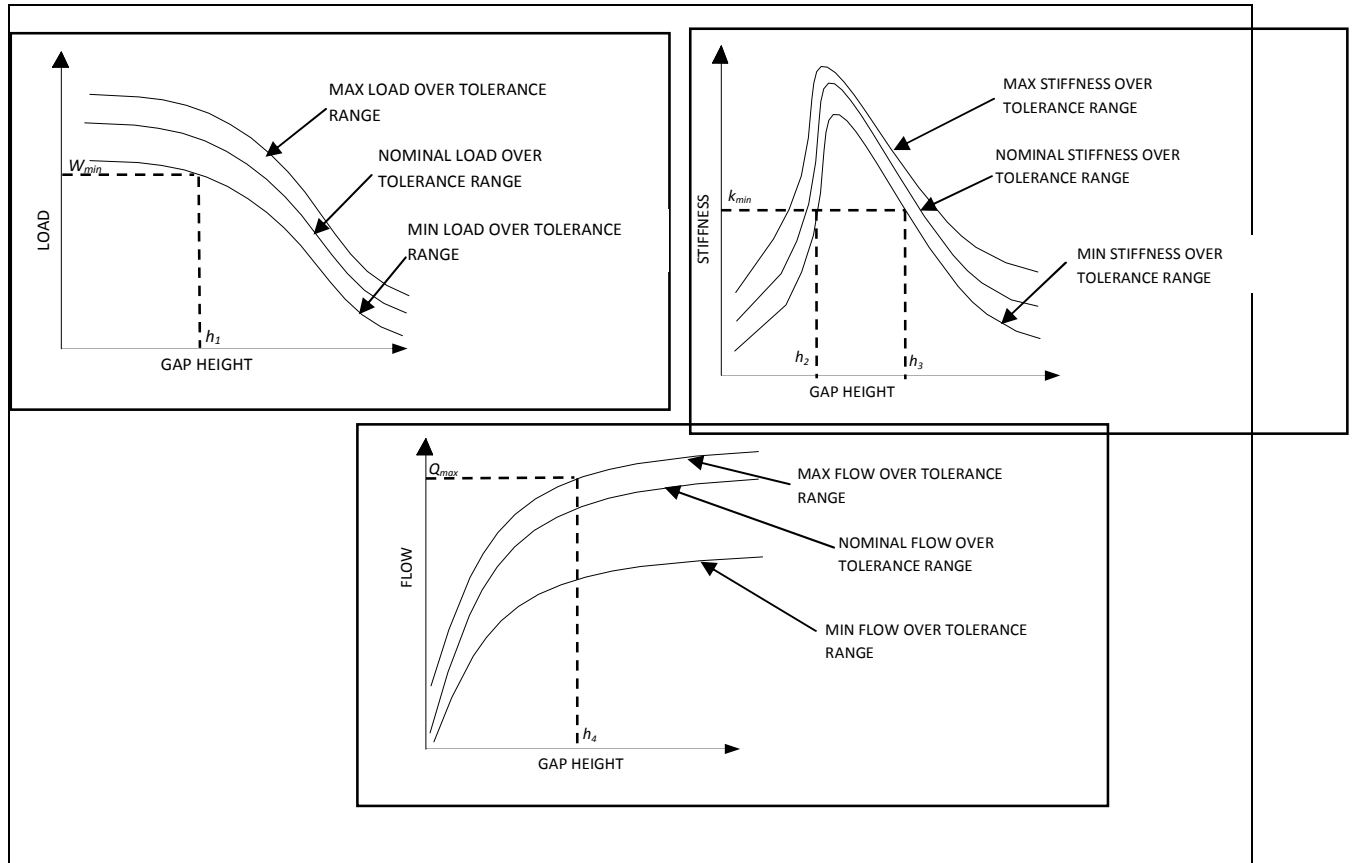
Figure 9. Illustrating how surface form error may impact on bearing performance

Note that having set the upper and lower bounds, it will not be possible to produce bearings with strange performances (such as negative stiffness). This ensures that the bearings at the extremes of manufacturing variability do not become critically unstable. Using this technique, bearings that perform well but are also insensitive to manufacturing variations can be distinguished.

8. Conclusions

Surface profile deviations within certain limits may significantly enhance the performance of 'flat' pad bearings. Thus a sensitivity analysis can be used as a tool to develop high performance flat pad aerostatic bearings. Current manufacturing techniques especially diamond turning in conjunction with high precision polishing make it possible to introduce the engineered surface profiles essential for producing high performance bearings. However bearings subjected to extreme deviations of form error can also exhibit deleterious stiffness properties. Thus a tight control of surface form variation during manufacturing is required. Also the optimization techniques for an air bearing must take account of the

sensitivity of bearing performance to surface form errors. This will result in the design of bearings robust to surface form deviation.
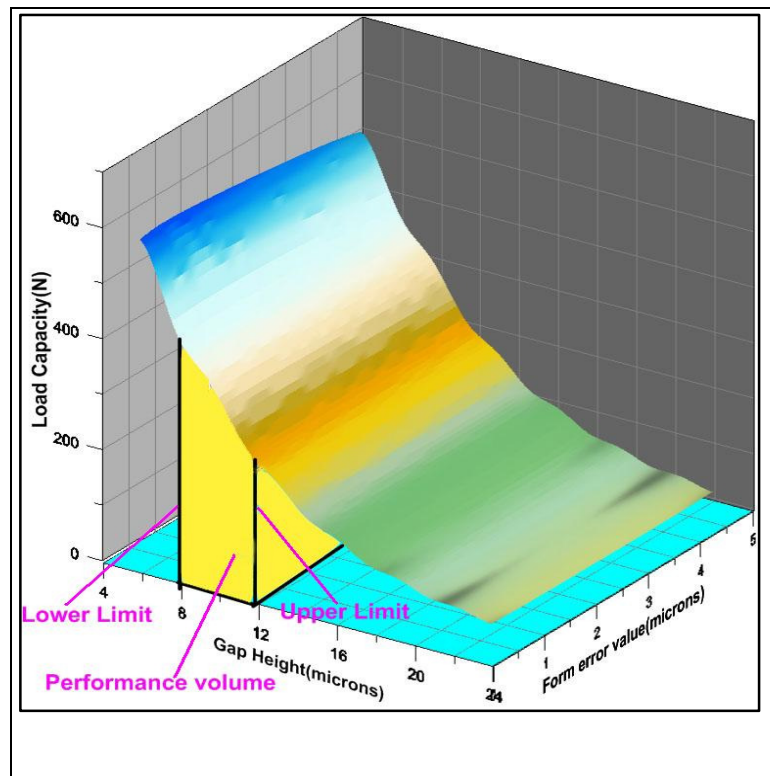
Figure 10. Definition of the load performance volume

The next step is to extend the current bearing analysis code to include a number of factors that will also have an impact on bearing performance. The current code does not take account of the fact that flow will be choked when pressure differentials are high. Also, the will be bearing designs within the design space that are inherently unstable for certain operating parameters. Both these factors could either limit the range of gap heights over which the bearing can be operated or make a particular bearing design unusable. In both cases, once the performance has been calculated by the bearing analysis code, accounting for it within the optimization algorithm is straight-forward.

Once these additional bearing performance factors have been accounted for, the current Pareto optimization technique can be extended to account for the sensitivity of the bearing design to errors in surface form. This will be done by using the performance volume concept as illustrated above. Also bearings with engineered surface profiles will be manufactured and tested to prove the concept of high performance bearings.

References

1. Park CH, Lee ES, Lee H. A review on research in ultra precision engineering at KIMM. International Journal of Machine Tools & Manufacture 1999; 39: 1793–1805.

2. Chenga H-B, Fenga Z-J, Chengb K, Wanga Y-W. Design of a six-axis high precision machine tool and its application in machining aspherical optical mirrors. International Journal of Machine Tools & Manufacture 2005; 45: 1085–1094.
3. Zhang Q D, Shan X C.   Dynamic characteristics of micro air bearings for Microsystems. Microsystem technologies 2008; 14 (2): 229-234.
4. TalkeFE. Tribology in magnetic recording technology. Industrial Lubrication and Tribology 2000; 52 (4): 157-165.
5. Fukumoto P, Allen N, Stonesifer G. Development of an air-bearing fan for space extravehicular activity (EVA) suit ventilation. In: Proceedings of the 22nd International Conference on Environmental Systems, 1992. Seattle: SAE; 1992. p 1-9.
6. v.Seggelena JK, Rosiellea PCJN, Schellekensa PHJ, Spaanb HAM, Bergmansc RH, Kottec GJWL. An Elastically Guided Machine Axis with Nanometer Repeatability. CIRP Annals - Manufacturing Technology 2005, 54 (1): 487-490.
7. Stout KJ, Pink EG. Orifice compensated EP gas bearings: the significance of errors of manufacture. Tribology International 1980;13(2):105–11.
8. Kwan Y-BP, Post JB. A tolerancing procedure for inherently compensated, rectangular aerostatic thrust bearings. Tribology International 2000; 33: 581–585.
9. Li Y, Ding H. Influences of the geometrical parameters of aerostatic thrust bearing with pocketed orifice -type restrictor on its performance. Tribology International 2007; 40: 1120-1126.
10. Chen X-D, HeX-M. The effect of recess shape on performance analysis of gas-lubricated bearing in optical lithography. Tribology International 2006; 39: 1336–1341.

11. Sharma RK, Pandey RK. Experimental studies of pressure distributions in finite slider bearing with single continuous surface profiles on the pads. Tribology International 2009; 42: 1040–1045.
12. Barrans SM, Bhat NJ. Manufacturing error sensitivity of flat pad air bearings. In: Proceedings of 9th International Conference and Exhibition on Laser metrology 2009, LAMDAMAP 2009. Teddington: EUSPEN; 2009.
13. Stout K J ; Barrans S.M. The design of aerostatic bearings for application to nanometre resolution manufacturing machine systems. Tribology International 2000; 33: 803–809.
14. Su Y-T, Liu S-H, Chen Y-W. A preliminary study on smoothing efficiency of surface irregularities by hydrodynamic polishing process. Wear 2001; 249: 808–820.
15. Rahman M, Lim HS, Neo KS, Senthil Kumar A, Wong YS, Li XP. Tool-based nanofinishing and micromachining. Journal of Materials Processing Technology 2007; 185: 2–16.
16. Chena S-T, Tsai M-Y, Lai Y-C, Liua C-C. Development of a micro diamond grinding tool by compound process. Journal of Materials Processing Technology 2009; 209: 4698–4703.
17. Stout KJ. Externally pressurized gas bearings. Penton Press, 2000.
18. Wang N, Chang YZ. Application of the genetic algorithm to the multi-objective optimization of air bearings. Tribol Lett 2004;17(2):119–28.
19. Jayson EM, Talke FE - Optimization of air bearing contours for shock performance of a hard disk drive. Trans ASME J Tribol 2005;127:878–83.
20. O'Hara MA, Bogy DB. Robust Design Optimization Techniques for Ultra-Low Flying Sliders. IEEE Transactions on Magnetics 1995; 31 (6): 2955–2957.
21. Zhu H, Bogy DB. Direct algorithm and its application to slider air-bearing surface optimization. IEEE Transactions on Magnetics 2002, 38 (5): 2168 – 2170.

22. Zhu H, Bogy DB. Hard disc drive air bearing design: modified DIRECT algorithm and its application to slider air bearing surface optimization. Tribol Int 2004;37:193–201.
23. Bhat N, Barrans SM. Design and test of a Pareto optimal flat pad aerostatic bearing. Tribology International 2008; 41: 181–188.
24. Wang N, Tsai C-M, Cha K-C. Optimum design of externally pressurized air bearing using Cluster OpenMP. Tribology International 2009; 42: 1180–1186.
25. Barrans S, Bhat N. Design of flat bed aerostatic bearings with the aid of finite element analysis. In: Proceedings of the 6th international Laser Metrology and Machine Performance conference, 2003. WIT Press, Southampton, 2003. pp. 361-370.
26. Al-Bender F, Van Brussel H. Symmetric radial laminar channel flow with particular reference to aerostatic bearings. Transactions of ASME 1992; 114: 630-636.
27. Liu Z-S , Zhang G-H, Xu H-J. Performance analysis of rotating externally pressurized air bearings. Proceedings of the Institution of Mechanical Engineers, Part J: Journal of Engineering Tribology 2009; 223 (4): 653-663.
28. Stout KJ, El-Ashkar S, Ghasi V, Tawfik M. Theoretical analysis of two configurations of flat pad aerostatic bearings using pocketed orifice restrictors. Tribology International 1993; 26 (4): 265-273.
29. Stout KJ, Rowe WB. Externally Pressurised Bearings - Design for Manufacture Including a tolerancing Procedure. Tribology 1974; August: 169 – 180.
30. Pink EG, Stout KJ. Design procedures for orifice compensated gas journal bearings based on experimental data. Tribology International 1978; February: 63-75.
31. Salem E, Khalil F. Choked flow in externally pressurized spherical gas bearings. Wear 1978; 47: 61–70.
32. Rahman M, Lim HS, Neo KS, Senthil Kumar A, Wong YS, Li XP. Tool-based nanofinishing and micromachining. Journal of Materials Processing Technology 2007; 185: 2–16.
33. Beaucamp A, Freeman R, Morton R, Ponudurai K, Walker DD. Removal of diamond-turning signatures on x-ray mandrels and metal optics by fluid-jet polishing. Proceedings of SPIE 2008; 7018.
34. Paula G. Automating lens manufacturing. Mechanical Engineering 1997; 119 (3): 88–91.
35. Chenga H-B, Fenga Z-J, Chengb K, Wanga Y-W. Design of a six-axis high precision machine tool and its application in machining aspherical optical mirrors. International Journal of Machine Tools & Manufacture 2005; 45: 1085–1094.
36. Katahira K, Ohmori H, Anzai M, Yamagata Y, Makinouchi A, Moriyasu S, Lin W. Development of large ultraprecision mirror surface grinding system with elid. In: 10th International Conference on Precision Engineering (ICPE) 2001, Yokohama, Japan, 10.1007/0-306-47000-4_156.
37. http://www.zeeko.co.uk/
38. Charlton P, Blunt L, Polishing Freeform implant surfaces using a 7 axis CNC polishing machine. In: Proceedings of 7th International Laser Metrology and Machine Performance Conference 2005. EUSPEN; 2005: 322-331.
39. Charlton P, Blunt LA. Surface and form metrology of polished "freeform" biological surfaces. Wear 2008; 264: pp 394–399.
40. Barrans SM, Yao S, Charlton P, Profiled surface aerostatic bearings. In: Proceedings of the 8th International Laser Metrology and Machine Performance conference, 2007. EUSPEN; 2007. p 242-251.
41. Thomas M, Sander M. Improving Optical Free-Form Production. Photonics Spectra 2006, September Issue.